J. Fluid Mech. (1987), *vol.* 175, *pp.* 85–96
Printed in Great Britain

Stability and heat transfer of rotating cryogens. Part 3. Effects of finite cylindrical geometry and rotation on the onset of convection

By J. M. PFOTENHAUER,† J. J. NIEMELA AND R. J. DONNELLY

Department of Physics, University of Oregon, Eugene, OR 97403, USA

(Received 25 March 1986 and in revised form 10 June 1986)

This report presents data describing convection in a rotating cylindrical Bénard cell filled with He I. In particular, convection modes are observed at Rayleigh numbers substantially below those predicted by linear stability analyses for a horizontally infinite layer. Both the Rayleigh numbers associated with the convective onset and the initial-slope measure of heat transport of these modes are found to depend on the rotation rate Ω and the aspect ratio Γ of the cell. A discussion of the relevant literature reveals that these convective modes are probably the same as those observed by Rossby (1969) and are reasonably well characterized by the recent analysis of Buell & Catton (1983) assuming asymmetric modes.

1. Introduction

In two previous reports, Lucas, Pfotenhauer & Donnelly (1983) (Part 1) and Pfotenhauer, Lucas & Donnelly (1984) (Part 2) we have described the stability and heat transfer of standard Bénard convection in a rotating system and have demonstrated that the experimental data generally support existing theories. In one major respect, however, the experimental data revealed some unexpected results which we intend to describe in this report in some detail. These results pertain to convective modes which occur at Rayleigh numbers less than the theoretical critical values for steady convection in a horizontally infinite layer, and which we have designated as 'subcritical' in Parts 1 and 2 of this series of papers. Recent linear analysis by Buell & Catton (1983), however, on the stability of convection in finite cylindrical containers subject to rotation suggests that this term may be inappropriate in describing our observations. We discuss this subject more fully in §4.

The apparatus and nomenclature used in this report have been discussed fully in Parts 1 and 2. In short, convective stability and heat transfer are measured in terms of the Rayleigh number Ra and the Nusselt number Nu respectively. In addition, we report the dependence of these variables on changes in a dimensionless rotation parameter $\Omega = \Omega_D d^2/\nu$, and on the aspect ratio $\Gamma = D/2d$ of our convection cells. Here, Ω_D is the dimensioned rotation rate and ν is the kinematic viscosity of the fluid contained in a cell of height d and diameter D. The values of Ω and Γ range from 0 to 3050 and from 1.97 to 7.81 respectively. The data we report here were taken with the upper boundary of our cell fixed at temperature $T_C = 2.63$ K, where the

† Present address: Applied Superconductivity Center, 1500 Johnson Drive, University of Wisconsin-Madison, Madison, Wisconsin 53706, USA.

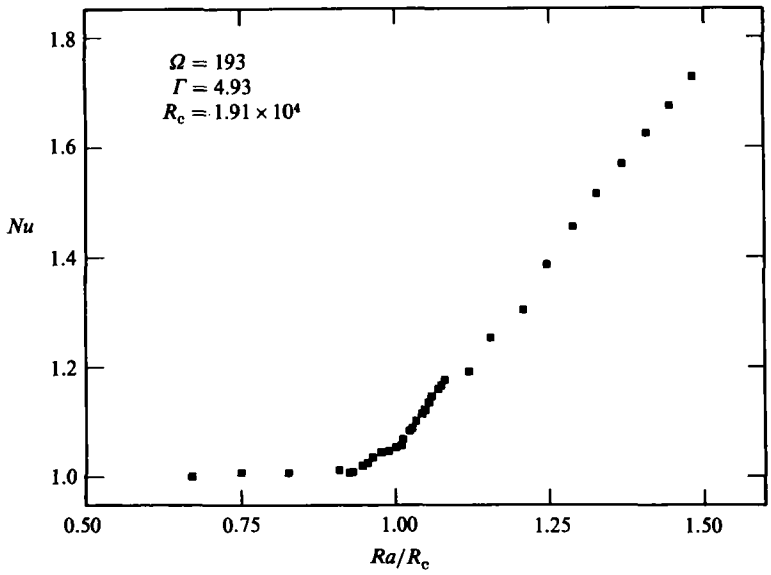

FIGURE 1. Evidence of convection at $R_{sc} < R_c$. The Nusselt number increases above unity at values of Ra below R_c.

Prandtl number Pr has the value 0.49. Parts 1 and 2 may be consulted for methods of data acquisition and experimental uncertainties.

Our discussion of the observation of steady convective modes below the expected infinite-layer onset is organized as follows. In §2 we describe the critical Rayleigh numbers associated with the onset of these modes. The corresponding heat transfer properties are given in §3. Section 4 contains a discussion of possible theoretical explanations for the observed modes and §5 contains concluding comments.

2. Onset of Convection

In general, measurements of the onset of steady convection at particular fixed values of T_C reveal that critical Rayleigh numbers $R_c(\Omega)$ fall below theoretical values for an infinite layer by a constant percentage. At $T_C = 2.63$ K, for instance, the measured values of $R_c(\Omega)$ all fall approximately 10% below theoretical values. This discrepancy is believed to be due to inaccurate values of the fluid parameters of helium I at that temperature. These measured values of $R_c(\Omega)$ are determined by a sudden rise in Nu above the conduction value of unity. However, as the rotation rate is increased beyond a critical value (as defined below) the experimental results are quite different: two increases in Nu are seen to occur for $Ra \leqslant R_c$ as shown in figure 1. The critical Rayleigh number for steady convection modes relevant to an infinite layer, $R_c(\Omega)$, which we assume is the same percentage below the theoretical value as when the rotation is 'slow', is still seen as the beginning of the major increase in Nu. But the first, smaller increase in heat transfer from the conductive state $Nu = 1$ appears to be associated with the onset of some other convective mode occurring for Rayleigh numbers $R_{sc} < Ra < R_c$, where R_{sc} denotes its onset. A number of possible explanations are given in §4, including the possibility that it results from a subcritical instability, e.g. from finite-amplitude effects. The position taken there is that it probably does not, although this question is by no means completely settled.

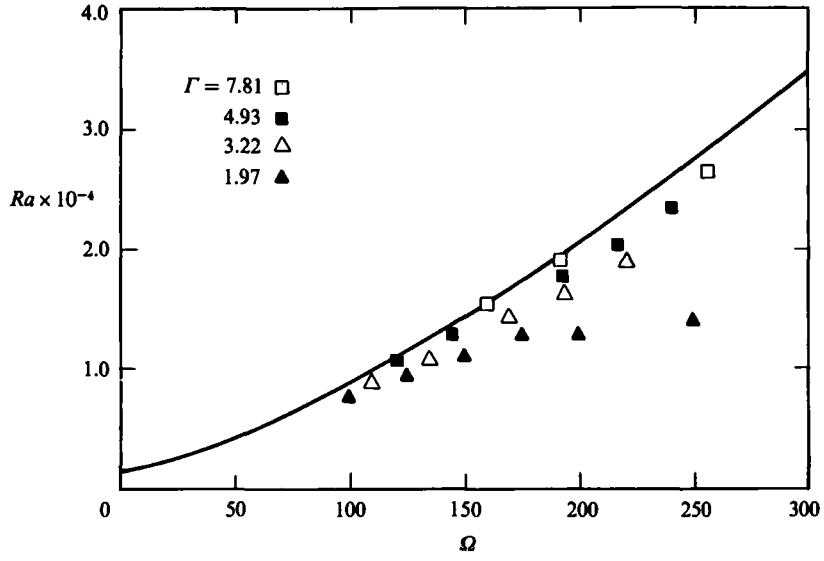

FIGURE 2. Variation in critical Rayleigh numbers $R_{sc} < R_c$ as a function of Ω with Γ as a parameter. The data give an approximate value for Ω_1 for each Γ.

The occurrence of steady convection at Rayleigh numbers substantially below those predicted for the infinite layer is found only above a certain rotation rate $\Omega = \Omega_1$, which in turn is found to depend on the aspect ratio Γ of the cell. In particular, these convective modes appear at lower rotation rates as Γ is decreased. Some effort was taken to discover the value of Ω_1 (for each Γ) above which these modes would be observed. The values of $\Omega_1(\Gamma)$ reported here are by necessity slightly larger than the 'true' critical rotation rates and are such that R_{sc} is clearly distinguishable from R_c. The scatter in Nu in this critical region required in practice that $R_c/R_{sc} > 1.05$ before this distinction could be made. Investigations of this type reveal that the value of Ω_1 for the case when $\Gamma = 7.81$ is less than the value of 200 reported in Lucas *et al.* (1983) and is closer to $\Omega_1 = 140$.

Measured values of R_{sc} in the range of $\Omega < 260$ for various values of Γ are shown in figure 2. The solid line in this graph represents a fit to the critical Rayleigh numbers identified in these runs. It is worth reminding the reader that the values of R_c defining this solid line were taken with the upper boundary of our cell controlled at temperature $T_C = 2.63$ K, and all fall about 10 % below the values predicted by linear stability theory. The apparent inaccuracy of the helium I fluid parameters mentioned above suggest that the absolute values of R_{sc} and R_c at any given Ω are not to be considered as important as their relative values.

In addition to the decrease in Ω_1 with decreasing Γ, it is found that, for a given value of Ω, values of R_{sc} also decrease with decreasing Γ. We have extended our measurements of R_{sc} with the smallest values of Γ (1.97) to large values of Ω and these results are shown in figure 3. A number of features of this figure deserve attention and these may be categorized according to values of Ω. At rotation rates below $\Omega \approx 850$, multiple values of R_{sc} are found (for fixed values of Ω). The spread in the measured values of R_{sc} at a particular rotation rate becomes quite large in the middle of this range of Ω, such that near $\Omega = 400$ the upper bound on R_{sc} is approximately 40 % greater than the lower bound.

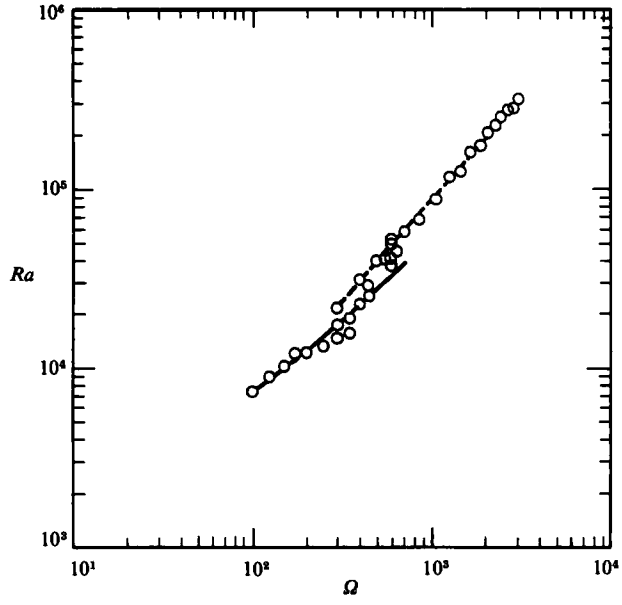

FIGURE 3. Critical Rayleigh numbers $R_{sc} < R_c$ measured with the $\Gamma = 1.97$ cell. The solid line represents the analysis of J. C. Buell (private communication) and the dashed line represents the fit $R_{sc} = 27.5\,\Omega^{1.18}$.

The cause of this indeterminency in R_{sc} is at present unknown. However a number of related facts have been established. As described in Part 1, the experimental protocol involves increasing the power to the cell in steps separated by an appropriately chosen waiting time. This time is determined by the vertical thermal-diffusion time (τ_D) associated with the height of the cell. Repeated measurements of R_{sc} with the waiting time varied from $1\tau_D$ to approximately $5\tau_D$ give identical results. One should note that the horizontal themal-diffusion time, which depends on the radius of the cell, is about 4 times larger than that related to the cell height. Denoting this time by τ_{Dh}, the waiting times are then in the range $0.25\tau_{Dh}$ to about $1.25\tau_{Dh}$.

When repeated measurements of R_{sc} are made within a few days of each other, the results are identical. In addition, the procedure used to set up an experimental run (including cool-down time, temperature control, and rotational control) is repeated in the same manner each time. However, measurements separated in time by about a month result in the range of R_{sc} values shown in figure 3. Presumably, there is a variable that we are unable to control which gives the observed variance in the values of R_{sc} at fixed Ω.

In the range of $\Omega > 850$, single values of R_{sc} are found for any given value of Ω. These are well described by the empirical fit $R_{sc} = 27.5\,\Omega^{1.18}$. It is also interesting to note that this fit passes through the upper bound on the values of R_{sc} measured in the range of $300 \leqslant \Omega \leqslant 850$ (see the dashed line in figure 3).

3. Heat Transfer

Various aspects of the initial convective modes occurring above $\Omega_1(\Gamma)$ have become evident through observation of relevant heat-transfer properties. Most notably, we find that more than one type of convection mode exists for $\Omega > \Omega_1(\Gamma)$ (and $Ra < R_c$),

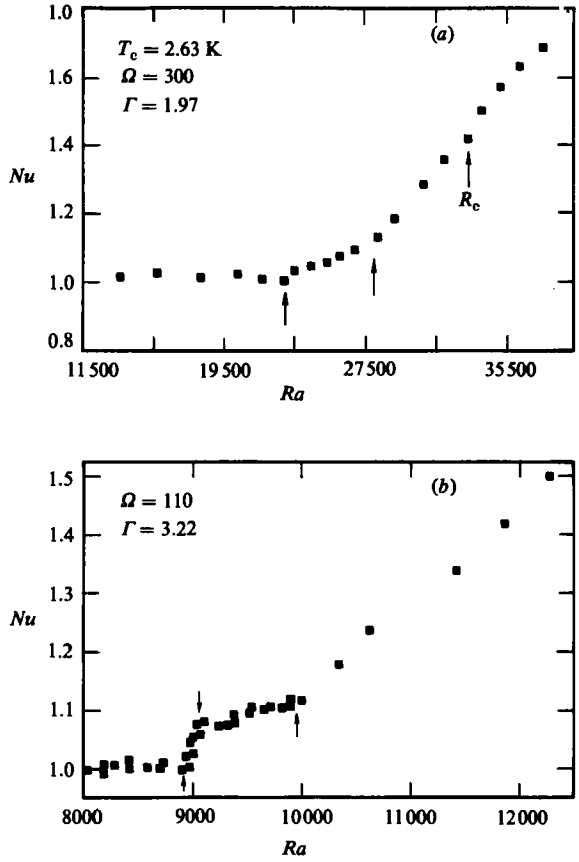

FIGURE 4. Two different heat-transfer sequences displaying various convection modes for $Ra < R_c$. The arrows mark the assumed transitions from one convection mode to another. The expected values of R_c for standard convection are also indicated.

and that their existence is determined by the aspect ratio Γ. In addition, the data suggest that more convective modes appear as Γ is decreased.

For the largest-aspect-ratio cell, and for all $\Omega > \Omega_1$, the heat-transfer characteristics are well typified by figure 1. In these, only one discontinuity in the heat-transfer data is observed below that associated with R_c. However, for the smaller-aspect-ratio cells, heat-transfer characteristics such as shown in figure 4(*a*) are sometimes observed. In these cases the heat-transfer slope increases discontinuously and dramatically at first, then changes discontinuously again, finally increasing discontinuously at a higher Rayleigh number, which is probably R_c. Yet another sequence of heat-transfer slopes is displayed in figure 4(*b*). For the smaller aspect ratio ($\Gamma = 1.97$) and in the range $200 < \Omega < 850$ both heat-transfer sequences shown in figure 4, as well as a number of other different sequences, are observed. Although this region is the same as that in which many different values of R_{sc} are measured, any correlation between the various heat-transfer sequences and the values of R_{sc} remains elusive.

In contrast, above a sufficiently large value of Ω (defined here as Ω_2), the heat-transfer data for the smaller-aspect-ratio cells are uniform and repeatable as were all the data for the $\Gamma = 7.81$ cell. The data suggest that as Γ is increased, $\Omega_2(\Gamma)$

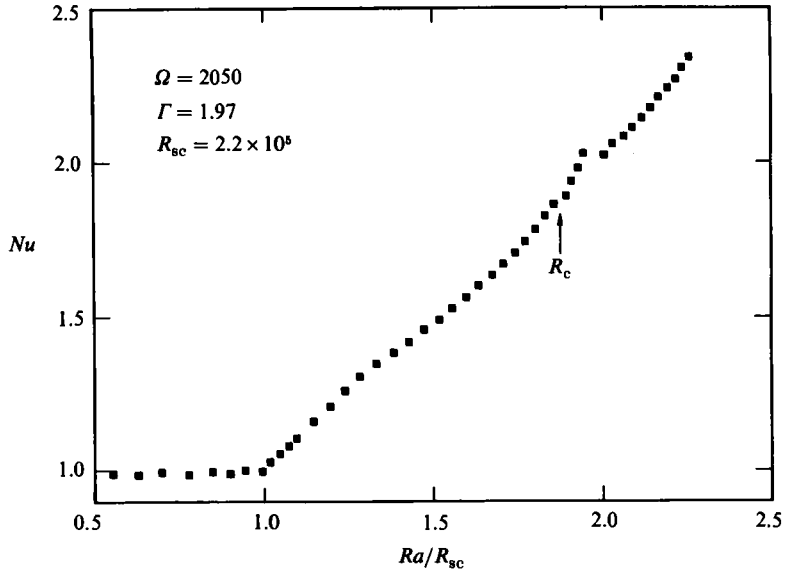

FIGURE 5. Convective heat transfer for typical mode observed above Ω_2. The sharp discontinuity above R_c is probably indicative of the skew-varicose instability.

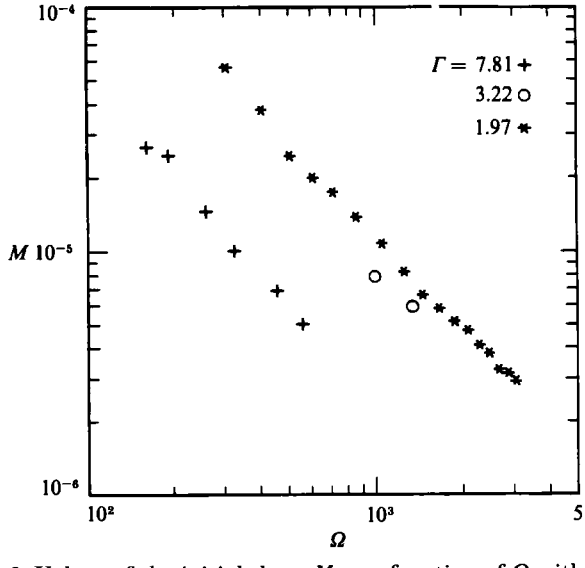

FIGURE 6. Values of the initial slope M as a function of Ω with Γ a parameter.

decreases such that when $\Gamma = 7.81$, $\Omega_2 \leqslant \Omega_1$. In the case of the $\Gamma = 1.97$ cell, Ω_2, ≈ 850 and the heat-transfer data above this rotation rate are typified by those shown in figure 5. This uniformity is notably true with respect to the discontinuities at large Ra/R_{sc}. We note that the value of R_c for the onset of steady convective flow in an infinite layer that is rotated at the same rate as the given in figure 5 is 4.59×10^5. The Rayleigh number 10% below this number is equivalent to a value of $Ra/R_{sc} = 1.88$ and is indicated in figure 5 by the arrow labelled R_c. All of the data taken for $\Omega > 850$ display similar discontinuities at the expected values of R_c. The

discontinuity seen at the larger value of Ra/R_{sc} (that is, above R_c) is also observed in all the data for $\Gamma = 1.97$ and $\Omega > 850$ and in fact appears similar in form to the supercritical feature seen in figure 1 where $\Gamma = 4.93$. The values of Ra/R_c at which these features are observed suggest that they may be indicative of the skew-varicose instability, consistent with the observations of Behringer, Gao & Shaumeyer (1983).

Another aspect of the convection modes obtained when $\Omega > \Omega_1(\Gamma)$, which is visible in the heat-transfer data, is the initial slope, or the initial increase in the heat transfer near the onset of convection. Using the variable $M = \mathrm{d}(Nu)/\mathrm{d}(Ra)$, defined in the range $R_{sc} < Ra < 1.25\,R_{sc}$ we find that the initial slope is dependent on both Ω and Γ. The variations in M when $\Omega < \Omega_2$, are difficult to classify owing to the variety of modes present, however some useful comments can be made concerning variations in M above Ω_2. Figure 6 displays the values of M plotted against Ω with Γ a variable parameter. The data follow a power law of the form $M = C\Omega^n$ where $n = -1.32 \pm .08$ and C is some function of Γ. Presently there is insufficient data to determine the form of this function beyond noting that C decreases as Γ increases.

Some points included in the $\Gamma = 1.97$ set of data extend the line to values of $\Omega < \Omega_2$ and these correspond directly to the points that fall on the dashed line in figure 3. Since the values of both R_{sc} and M produced in these runs below Ω_2 obey the same power laws as those produced in runs above Ω_2, they are probably determined by the same convection mode.

4. What is the origin of convection at $Ra < R_c$?

Convection at Rayleigh numbers less than $R_c(\Omega)$ in a rotating Bénard-convection system is not a new phenomenon. Indeed, of the instabilities intrinsic to rotation, the Kuppers–Lortz instability is the only one that does not produce convection at $Ra < R_c$. In the light of this, it is important to distinguish which of the instabilities, if any, are responsible for the convective modes described in the previous section.

4.1. *Overstability*

The theories describing overstability (see, for example, Chandrasekhar 1961) predict that if the Prandtl number Pr of a fluid is low enough, convection can occur at values of Ra (designed as Ra_0) below $R_c(\Omega)$, and that the convective amplitude will grow and decay as oscillations with a characteristic frequency σ. The upper bound in Pr for this type of convection is 0.67 and as this limit is approached from below, the lowest value of Ω above which overstability can occur increases dramatically. Also, if overstable flows are possible for two different values of Pr (both less than 0.67) at the same Ω, then the ratio Ra_0/R_c will be smaller for the lower value of Pr (see Clever & Busse 1979, figure 2). The range of Pr readily accessible for helium I is $0.49 < Pr < 0.76$, with the lowest value at the temperature of 2.63 K. Thus, if overstability were the mechanism responsible for the flows observed at $\Omega > \Omega_1$ in this study, one would expect these flows to be present at the lowest value of Ω when $Pr = 0.49$ ($T_C = 2.63$ K), and not present at any value of Ω for $Pr = 0.76$ ($T_C = 2.186$ K).

The results presented by Clever & Busse (1979) suggest that even for $Pr = 0.49$ a value of Ω well in excess of 100 is needed for overstable flows to exist. Indeed F. H. Busse (private communication) puts the lower bound on Ω, for the case $Pr = 0.4$, near 1500. We find, however, that convective modes exist for $Ra < R_c$ when $Pr = 0.76$ as well as when $Pr = 0.49$. Further, the ratio $R_{sc}/R_c = 0.853$ for the same rotation rate of $\Omega = 452$ for both Prandtl numbers.

We believe that it is unlikely that overstability is the mechanism responsible for the onset of convection at R_{sc}.

4.2. *Finite-amplitude effects of two-dimensional flows*

Veronis (1968) has described in detail predictions of a form of two-dimensional Bénard convection that could appear in a horizontally infinite layer at Rayleigh numbers below the critical values predicted by linear stability theory for either steady or time-dependent (overstable) convection. These predictions appear in his theory as a result of allowing for finite-amplitude disturbance terms to be present in the perturbation equations rather than just the infinitesimal disturbance terms allowed by linear stability theory. Veronis' theory shows, however, that these finite-amplitude flows can appear only if $Pr < 1.414$.

An experimental study, contemporary with the theory of Veronis, was reported by Rossby (1969) and displayed subcritical convection in water. The finite-amplitude theory was unable to explain this behaviour, however, since Pr for water is approximately 6.8. The convective motions observed in the present study have a number of characteristics in common with those reported by Rossby. These modes, also observed in rotating cylindrical containers, display values of R_{sc} which fall further below R_c as Ω is increased and show a relatively small increase in Nu for aspect ratios $\Gamma > 2$. Also, when only one convection mode is observed below R_c, the second change in the heat-transfer slope occurs at Rayleigh numbers equal to $R_c(\Omega)$ within experimental uncertainty. Further, when the height of the container is increased, the slope of the heat-transfer data below R_c increases. The present study shows more generally that this heat-transfer slope increases when Γ is decreased, either by increasing the height with fixed radius or by decreasing the radius with fixed height. These similarities suggest that the convection reported here in helium I ($Pr \approx 0.6$) for $\Omega > \Omega_1$ is the same as that observed by Rossby (1969) in water ($Pr \approx 6$). Since the theoretical work of Veronis describing the finite-amplitude convection predicts completely different results above and below $Pr = 1.414$, it is not clear that finite-amplitude effects can provide an explanation of the convection we observe to occur for $Ra \geqslant R_{sc}$.

4.3. *Centrifugal effects*

When a rotating layer of fluid is heated from below and cooled on top (as in rotating Bénard convection), some small radial flow of the fluid is induced. This occurs since the centrifugal force on the colder, heavier fluid on top is greater than the same force on the warmer, less dense fluid on the bottom. Flow is induced away from the centre of the top of the fluid layer, downwards along the vertical walls, and inward toward the centre of the bottom of the fluid layer. Koschmieder (1967) demonstrated that this effect created a series of convective rolls, the first appearing next to the outer vertical wall of his cylindrical Bénard cell. These convection rolls appeared at Rayleigh numbers below $R_c(\Omega)$.

The quantity $\Omega_D^2 D/2g$ (or the Froude number F) provides a measure of the ratio of centrifugally induced accelerations to buoyancy-induced accelerations. The conditions under which Koschmieder observed these centrifugal flows were such that $F = 0.25$. Although at the time of the writing of Lucas *et al.* (1983), our data gave values of F two orders of magnitude lower than Koschmieder's, the suspicion that our convective flows might be subcritically induced by centrifugal effects could not be ruled out. It was decided that the most direct method of investigating this possibility was to change the diameter of the container. Thus, for the same Froude

number and the same magnitude of centrifugal effect, a decrease in D would imply an increase in Ω. Equivalently, it was expected that a decrease in D would increase the lowest value of Ω above which flow for $Ra < R_c$ could be observed. The data presented in figure 2 show that the opposite effect is observed; the decrease in D results in a decrease in the minimum value of Ω for observing these flows.

A number of papers by Homsy & Hudson (1969, 1971*a*, *b*, 1972) have discussed the conditions theoretically required for centrifugal effects to cause convection in cylindrical containers. The condition $F \gg 1$ is shown to ensure the presence of centrifugal effects, but a less stringent requirement given (Homsy & Hudson 1971*b*) is that $F \gg \lambda\gamma$. Here $\lambda = (1/8\sqrt{2})\,[Pr\,\beta_p\,\Delta T\Omega^{\frac{1}{2}}]$, which is a ratio of convective to conductive heat transfer in the core of the fluid layer, and $\gamma = 2\Gamma$. An attempt was made by Homsy & Hudson (1971*b*) to explain Rossby's subcritical data by centrifugal effects. They concluded that the parameter range of Rossby's data did not fit the requirement $F \gg \lambda\gamma$. For the parameter range covered in this study, we find that $F/(\lambda\gamma)$ does not exceed 1.77 and that $F \gg 1$ for all of the convective data obtained for $Ra < R_c$.

It is interesting to observe here that a recent experimental study (Buhler & Oertel 1982) demonstrates that when the Froude number exceeds unity, centrifugal accelerations cause convective flows. Buhler & Oertel obtain values of $F > 1$ at low values of Ω by using high-viscosity oil as the working fluid. Thus for rotation rates such that $\Omega_D^2 D/2g$ is greater than unity, $\Omega_D d^2/\nu$ is still small. In this same report, however, nitrogen gas (low viscosity) is used to obtain larger values of Ω while $F > 1$. The results with nitrogen gas, given for $\Omega \leqslant 158$, do not display any convection at $Ra < R_c$. This is possibly because the containers were rectangular, although our results suggest that smaller aspect ratios and higher rotation rates than those used in their experiments would probably be necessary in order to observe this effect.

In addition to the above considerations, we have carried out a novel experiment to investigate centrifugal effects. Helium I has the property that in a limited temperature range just above the lambda point, the thermal-expansion coefficient is negative. By controlling T_C at 2.1725 K and maintaining the bottom of the cell at $T_F = 2.1795$ K by adding heat, it is possible to create a *stable* density gradient that is equal (and in some cases greater) in magnitude to those that existed when convective flows below R_c are observed. Ω was then incremented up to 1000 and the heat transfer of the system was observed. Any increase in the heat transfer could only be due to centrifugal effects and this is monitored by looking for changes in the applied heat flux ($W_F = 10.5$ μW) required to maintain T_F at 2.1795 K. Fluctuations in W_F are limited to 0.02 μW, and no deviations from the mean value of 10.5 μW were observed over the entire range of Ω investigated. These fluctuations in W_F are equivalent to fluctuations in Nu of order 0.002, and these are smaller than the smaller changes in Nu observed in convective flows below R_c.

In considering the implications of this last check, it becomes clear that if centrifugal effects were responsible for the convective onset at $R_{sc} < R_c$, values of R_{sc} would not increase as Ω is increased. Indeed, one would expect an increase in Ω to generate more centrifugal flow for the same density gradient, or equivalently, for the same ΔT and thus the same value of Ra. However, as is clear in figures 2 and 3, an increase in Ω requires large values of Ra to produce convective flow below R_c.

We conclude from the above considerations that centrifugal effects do not provide a reasonable explanation for the convective modes observed for $R_{sc} < Ra < R_c$.

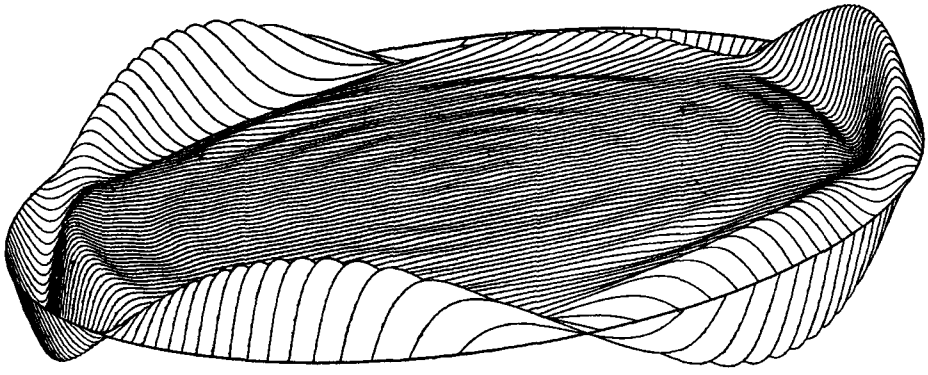

FIGURE 7. Depiction of the $m = 3$ asymmetric convection mode. The vertical displacement represents the amplitude of convection. Note that the small wiggles in the interior are not physical but indicate the approximate size of the numerical error. (Courtesy of J. C. Buell.)

4.4. *Asymmetric modes*

In a recent study, Buell & Catton (1983) discuss the stability of a set of asymmetric convection modes in rotating cylindrical containers. The convective pattern, described in more detail by Buell (1981), is basically one of concentric rolls, but slightly different from the usual symmetric type observed in previous studies (see, for instance, Koschmieder 1967). Buell describes the asymmetric modes as having the largest amplitude next to the vertical walls (and thus sensitive to the thermal properties of the walls), and being asymmetric with respect to the azimuth of the convective amplitude. Different modes thus have different numbers of amplitude nodes around the azimuth of the convection roll. An example of the $m = 3$ mode is shown in figure 7.

Buell & Catton (1983) show that these asymmetric modes produce steady convection at Rayleigh numbers below the corresponding critical values given by linear stability theory for the horizontally infinite layer and that these values depend on Γ as well as on Ω. The parameter range covered is $0 \leqslant \Omega \leqslant 700$ and $0.2 \leqslant \Gamma \leqslant 2.0$, and the Rayleigh numbers for a given mode are shown to increase with Ω for a fixed Γ and to increase with Γ for a fixed Ω. In fact, for a given sidewall conductance, rotation rate and mode number, the latter is valid only for aspect ratios greater than some minimum, which appears to be slightly less than unity for conditions similar to those encountered in our experiments. Recent results obtained by J. C. Buell (private communication) modelling the size and thermal conductivity of the sidewalls of our $\Gamma = 1.97$ container are displayed as the solid line in figure 3.

The heat-transfer properties of these asymmetric modes have not yet been calculated. However, the aspect-ratio dependence of R_{sc}, the magnitude of the effect of these asymmetric modes on values of R_{sc}/R_c, and the multiplicity of possible modes are in qualitative agreement with the experimental results, at least at moderate rotation rates, as shown in figure 3.

5. Conclusions

Both the stability and the heat transfer of the convective flows observed for Rayleigh numbers $R_{sc} < Ra < R_c$ in this study have been shown to depend on the rotation rate Ω and on the aspect ratio Γ. The rotation rate was shown to influence

these convective modes in a manner similar to its influence on standard convection in a horizontally infinite layer. As Ω increases, so do values of R_{sc}; however these fall further below the corresponding values of R_c as Ω is increased. Also, as Ω increases, values of M decrease, indicating the constraining influence of rotation on the convective flows. For one mode, values of both R_{sc} and M obey power laws in Ω.

In addition, we find that the following characteristics are true as Γ is decreased. Convection below R_c becomes distinguishable from convection at $Ra > R_c$ for lower values of $\Omega = \Omega_1$; for a given value of $\Omega > \Omega_1$ values of R_{sc} decrease while values of M increase; and the domination of a single convective mode below R_c occurs above a larger value of $\Omega = \Omega_2$.

For the rotation range $\Omega_1 \leqslant \Omega \leqslant \Omega_2$, we are at present unable to determine or regulate the onset and/or sequence of convection modes that appear. The onset and sequence of modes do not appear to be influenced by variations in the waiting time between changes of the input power.

Finally, we have shown that the existence of convective modes below R_c is insensitive to the Prandtl number and we are therefore not inclined to appeal to either overstability or finite-amplitude effects as likely mechanisms for the observed instabilities. For a number of reasons, centrifugal effects are also excluded. In comparing the characteristics of our data with the asymmetric modes described by Buell & Catton (1983) we find that they provide a reasonable explanation for our results in the range of Ω shown in figure 3. However we cannot rule out the occurrence of finite-amplitude convection. This could be explored in the future by means of detailed hysteresis measurements.

We are indebted to Professor G. M. Homsy and F. Busse for discussions of this problem. This research was supported by the National Science Foundation Heat Transfer Program under grant MEA 83-20402.

REFERENCES

Behringer, R. P., Gao, H. & Shaumeyer, J. N. 1983 Time dependence in Rayleigh–Bénard convection with a variable cylindrical geometry. *Phys. Rev. Lett.* **50**, 1199.

Buell, J. C. 1981 The effects of rotation and wall conduction on the stability of a fully enclosed fluid heated from below. M.S. thesis, University of California, Los Angeles.

Buell, J. C. & Catton, I. 1983 Effects of rotation on the stability of a bounded cylindrical layer of fluid heated from below. *Phys. Fluid* **26**, 892.

Buhler, K. & Oertel, H. 1982 Thermal cellular convection in rotating boxes. *J. Fluid Mech.* **114**, 261.

Chandrasekhar, S. 1961 *Hydrodynamic and Hydromagnetic Stability*. Clarendon.

Clever, R. M. & Busse, F. H. 1979 Nonlinear properties of convection in rolls in a horizontal layer rotating about a vertical axis. *J. Fluid Mech.* **94**, 609.

Homsy, G. M. & Hudson, J. L. 1969 Centrifugally driven thermal convection in a rotating cylinder. *J. Fluid Mech.* **35**, 33.

Homsy, G. M. & Hudson, J. L. 1971*a* The asymptotic stability of a bounded rotating fluid heated from below: conductive basic state. *J. Fluid Mech.* **45**, 353.

Homsy, G. M. & Hudson, J. L. 1971*b* Centrifugal convection and its effect on the asymptotic stability of a bounded rotating fluid heated from below. *J. Fluid Mech.* **48**, 605.

Homsy, G. M. & Hudson, J. L. 1972 Stability of a radially bounded rotating fluid heated from below. *Appl. Sci. Res.* **26**, 53.

KOSCHMIEDER, E. L. 1967 On convection on a uniformly heated rotating plane. *Beitr. Z. Phys. Atmos.* **40**, 216.

KUPPERS, G. & LORTZ, D. 1969 Transition from laminar convection to thermal turbulence in a rotating fluid layer. *J. Fluid Mech.* **35**, 609.

LUCAS, P. G. J., PFOTENHAUER, J. M. & DONNELLY, R. J. 1983 Stability and heat transfer of rotating cryogens. Part 1. Influence of rotation on the onset of convection in liquid ^{4}He. *J. Fluid Mech.* **129**, 251.

PFOTENHAUER, J. M., LUCAS, P. G. J. & DONNELLY, R. J. 1984 Stability and heat transfer of rotating cryogens. Part 2. Effects of rotation on heat transfer properties of convection in liquid ^{4}He. *J. Fluid Mech.* **145**, 239.

ROSSBY, H. T. 1969 A study of Bénard convection with and without rotation. *J. Fluid Mech.* **36**, 309.

VERONIS, G. 1968 Large-amplitude Bénard convection in a rotating fluid. *J. Fluid Mech.* **31**, 113.